

# DNA Conjugated SWCNTs Enter Endothelial Cells via Rac1 Mediated Macropinocytosis

Santanu Bhattacharya,<sup>†</sup> Daniel Roxbury,<sup>‡</sup> Xun Gong,<sup>†</sup> Debabrata Mukhopadhyay,<sup>\*,†,§</sup> and Anand Jagota<sup>\*,‡</sup>

<sup>†</sup>Department of Biochemistry and Molecular Biology, Mayo Clinic, Rochester, Minnesota, 55905, United States

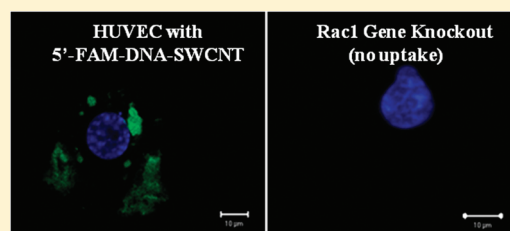
<sup>‡</sup>Department of Chemical Engineering and Bioengineering Program, Lehigh University, Bethlehem, Pennsylvania 18015, United States

<sup>§</sup>Department of Biochemistry and Molecular Biology and Biomedical Engineering, Mayo Clinic, Rochester, Minnesota 55905, United States

## S Supporting Information

**ABSTRACT:** Several applications of single-walled carbon nanotubes (SWCNT) as nanovectors in biological systems have been reported, and several molecular pathways of cellular entry have been proposed. We employed transmission electron microscopy, confocal fluorescent microscopy, and UV-vis spectroscopic analysis to confirm the internalization of DNA-SWCNT in human umbilical vein endothelial cells. Additionally, by using pharmacological inhibitors as well as genetic approaches, we have found that SWCNT is endocytosed through Rac1- GTPase mediated macropinocytosis in normal endothelial cells.

**KEYWORDS:** DNA-SWCNT, nanotubes, HUVEC, endothelial, internalization, pinocytosis



By virtue of their high surface area and tunable properties, biologically compatible nanomaterials have recently opened up a number of potential biomedical applications in sensing, imaging, and targeted intracellular delivery. Functionalized single-walled carbon nanotubes (SWCNTs) are a prime example due to their unique optical and physical properties.<sup>1</sup> Molecules can be attached to an SWCNT covalently or noncovalently; the latter of the two methods generally retains the SWCNT's optical integrity (NIR photoluminescence signals).<sup>2</sup> Cargo bound to SWCNTs have included antibodies,<sup>3</sup> chemotherapy drugs,<sup>4</sup> single-stranded DNA (ssDNA),<sup>5</sup> siRNA,<sup>6,7</sup> and short peptides.<sup>8</sup> Much effort has also been expended in developing conjugated SWCNTs as imaging and sensing entities in living organisms such as using fluorescence,<sup>9–11</sup> Raman,<sup>3,12,13</sup> and photoacoustic<sup>14</sup> techniques after substrate binding. In addition, there is considerable interest in understanding the potential health risks associated with carbon nanomaterials. Thus, it is vital to study their interactions at the cellular and molecular level. The biocompatibility of functionalized SWCNTs is strongly correlated with the nature of the surface conjugation. For example, a well-coated biopolymer-conjugated SWCNT yields relatively low levels of toxicity.<sup>6,15,16</sup> Long multiwalled CNTs (>10  $\mu\text{m}$  in length) have been found to promote carcinogenesis when administered through intraperitoneal injection.<sup>17–19</sup> However, far reduced toxicity is seen in CNTs less than 1  $\mu\text{m}$  in length.<sup>18</sup>

Nanomaterial uptake by cells may take place through numerous different mechanisms; these can broadly be classified as phagocytosis, receptor mediated endocytosis, and pinocytosis.

Phagocytosis facilitates the uptake of large particles by utilizing cell surface receptors.<sup>20</sup> Receptor mediated endocytosis is a distinct mechanism where internalization of receptor and its ligand is carried within clathrin-coated or uncoated vesicles.<sup>21,22</sup> Endocytosis of various membrane receptors may also occur via lipid rafts,<sup>23</sup> which enable the internalization of receptors, adaptors, regulators, and other downstream proteins as a signaling complex. Moreover, sometimes it may be accompanied by caveolae-mediated entry. Caveolae are involved in plasma membrane invaginations 50–80 nm in size including cholesterol and sphingolipids, receptors and caveolins.<sup>23,24</sup> On the other hand, clathrin-coated pits of 100–200 nm have been shown to be associated with the key protein clathrin and other scaffold proteins such as AP-2 and eps15.<sup>25</sup> Pinocytosis can take place through two different pathways, namely micropinocytosis and macropinocytosis. The micropinocytosis variety involves the uptake of particles no larger than 0.1  $\mu\text{m}$  in diameter whereas macropinocytosis is carried out with relatively large vesicles (0.2–5  $\mu\text{m}$  in diameter). It is the result of cell surface membrane ruffles folding back on the plasma membrane. Macropinosomes are not coated with clathrin or caveolin but encircled by actin in its early stages. Macropinocytosis provides an efficient process for nonselective uptake of nutrients and solute macromolecules.<sup>26</sup>

**Received:** November 17, 2011

**Revised:** January 26, 2012

**Published:** February 29, 2012

Several mechanisms have been proposed and studied for CNT internalization into cells. It has been shown that protein- or DNA-coated SWCNTs can pierce cells via energy-dependent endocytosis<sup>27–30</sup> and also via an energy-independent nonendocytotic pathway,<sup>31,32</sup> involving the insertion and diffusion of CNTs through the lipid bilayer of the cell membranes. Moreover, there are reports that SWCNTs can enter cells such as macrophages.<sup>33,34</sup> An active endocytotic pathway was hypothesized and further investigated using a single-particle fluorescence tracking method<sup>29</sup> to explore rates of endo- and exocytosis. Another study hypothesizes a clathrin-dependent endocytosis mechanism for the uptake of 15-base random DNA-CNTs.<sup>28</sup> CNTs have also been reported to directly enter living cells through spearing of the cell membrane.<sup>35</sup> Single-stranded DNA-SWCNT hybrid cellular uptake experiments have shown SWCNT accumulation in perinuclear endosomes of murine myoblast stem cells,<sup>36</sup> but these hybrids did not enter the nuclear envelope. Possibly, the diversity of proposed mechanisms is due to different surface modifications of SWCNTs as well as the differences in experimental cell types. Much remains to be understood in SWCNT uptake and its relationship with known endocytic pathways.

In this study, we have systematically explored several modes of proposed DNA-coated SWCNT cellular uptake in the human umbilical vein endothelial cell line (HUVEC), a primary normal cell extensively used for exploring endothelial cell functions. Cellular entry of DNA-SWCNT hybrids is confirmed by transmission electron microscopy. We have thoroughly explored the possibility of SWCNT internalization by clathrin, caveolae, macropinocytosis and microtubules associated pathways with the aid of five known classical pharmacological inhibitors. The effects of these inhibitors on the DNA-SWCNT uptake have been monitored quantitatively by laser scanning confocal fluorescence microscopy and near-infrared UV/vis spectroscopy. Actin polymerizations emerge as the key mechanism for this DNA-SWCNT hybrid endocytosis in endothelial cells. The gene *Rac1* plays an important role in actin polymerization near the plasma membrane, regulating macropinocytosis. We use a dominant negative *Rac1* (*Rac1-T17DN*) to down regulate DNA-SWCNT uptake, confirming the uptake mechanism. These findings provide information on the specific endocytic pathway that DNA-coated SWCNT employ to enter endothelial cells. Given the importance of endothelial cells in the transfer of agents between blood and tissue, this understanding can serve to improve the efficacy of SWCNT associated sensors and drug delivery vectors for the diagnosis and treatment of cancer.

As cytotoxicity is still a major issue with the usage of SWCNT we have thoroughly tested the viability of DNA-SWCNT conjugates in HUVEC cells. Details are described in Supporting Information, Section S1. Briefly, we have found that cellular viability, defined as cells maintaining the ability to metabolize MTS, decreases as a function of both incubation time and DNA-SWCNT concentration. At an extracellular concentration of 2  $\mu\text{g}$  SWCNT/mL, cellular viability was found to be greater than 80% in all samples up to and including 72 h of incubation (see Supporting Information Figure S1). Subsequent incubation studies have been performed at this particular concentration.

To visually confirm the uptake of DNA-SWCNT, cells were first examined by transmission electron microscopy (TEM). Figure 1 demonstrates that SWCNTs are indeed taken up by

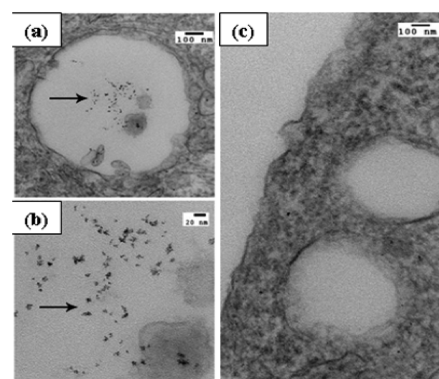


**Figure 1.** Visualization of DNA-SWCNT by transmission electron microscopy. (a,b) Transmission electron microscopy (TEM) images of HUVEC cells incubated with DNA-SWCNTs. Intracellular congregation, particularly inside the vacuoles, is evident in SWCNT-incubated samples, not seen in the control sample (c).

the cells after 6 h of incubation. In cellular vacuoles, clear accumulations of SWCNTs are found (localized black regions), which are absent in the control sample (Figure 1). The aggregation of SWCNTs suggests that they have been stripped of their amphiphilic DNA coating. Once stripped, CNTs tend to clump together due to hydrophobic attraction and their high aspect ratios.<sup>37,38</sup>

To identify the pathway for DNA-SWCNT uptake into the HUVEC cells, a pharmacological inhibition study is performed using different inhibitors which include chlorpromazine,<sup>39,40</sup> nystatin,<sup>39,41</sup> amiloride,<sup>39,42</sup> cytochalasin D,<sup>39,43</sup> and nocodazole.<sup>39,44</sup> Chlorpromazine is used to inhibit pit formation by clathrin relocation at the endosomes. Nystatin acts as inhibitor for caveolin pit formation. Amiloride and cytochalasin D are both used to inactivate macropinocytosis. Amiloride inhibits  $\text{Na}^+/\text{H}^+$ -ATPase exchangers whereas cytochalasin D helps in actin depolymerization for membrane extension. On the other hand, Nocodazole is used to hinder tubulin subunit polymerization and also to obstruct endosome trafficking. (See Supporting Information Section S2 (Table S1) for more information.)

Uptake was monitored by laser scanning confocal microscopy using 5'-FAM-fluorophore labeled DNA to create its hybrid with SWCNT. A control experiment has been performed to ensure that in the absence of SWCNT 5'-FAM-DNA does not enter the cells (see Supporting Information Section S3). Therefore, measured intracellular fluorescence intensity can be taken as a proxy for the quantity of SWCNT ingested by the cell. Note, however, that its spatial distribution is not necessarily indicative of SWCNTs' spatial location inside the cell since the 5'-FAM-DNA might well be partially or fully stripped off the SWCNT once both have entered the cell. Figure 2 shows micrographs with the nucleus, stained in blue, and 5'-FAM-DNA-SWCNT, indicated by green, under the influence of different drugs corresponding to various endocytotic pathways for DNA-SWCNT uptake. A confocal z-stack image for HUVEC incubation with DNA-SWCNT in the absence of drug inhibitors is shown in Figure 2e. It is known that SWCNTs can adsorb onto the plasma membrane prior to internalization.<sup>29</sup> However, the quantity of cell-internalized SWCNTs is so much greater than what could be accommodated on the plasma membrane that fluorescence of the former overwhelms any signal from the latter. Comparing images from different drug treatment with the control, as

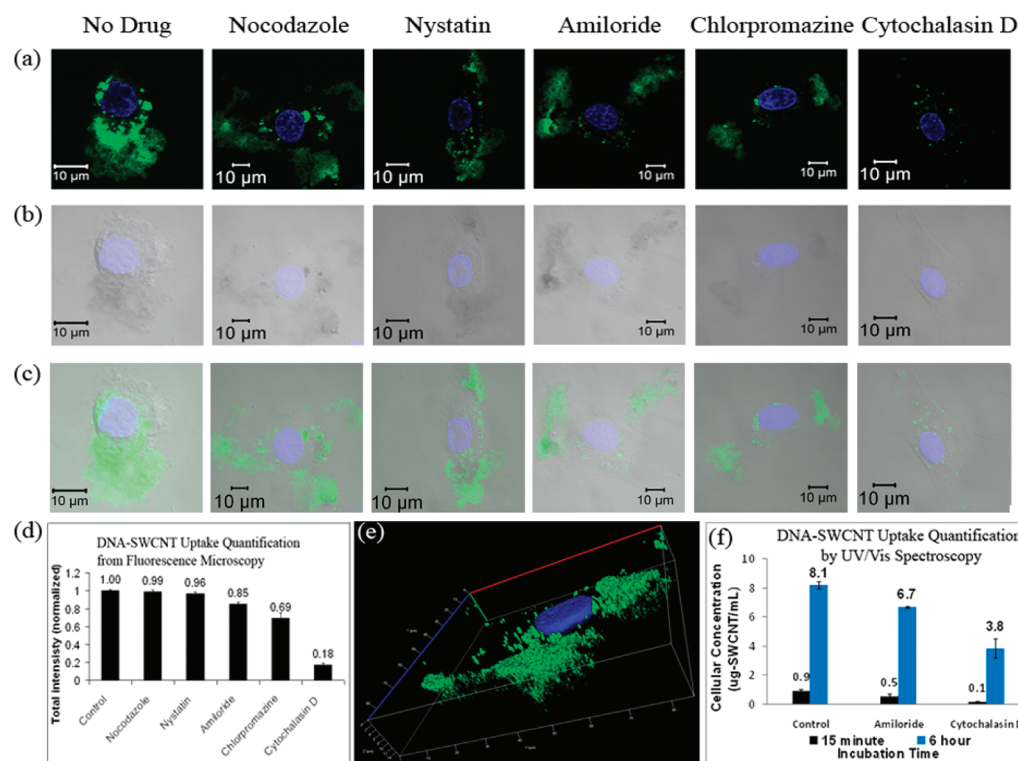


**Figure 2.** Comparison of DNA-SWCNT uptake on pharmacological inhibition study by laser scanning confocal microscopy. Phase contrast confocal imaging after application of different pharmacological inhibitors. DAPI (blue) is used for nucleus staining. The green color represents 5'-FAM dye conjugated to the DNA used in DNA-SWCNT hybrid production. (a) Images illustrating the presence of 5'-FAM-DNA-SWCNT inside the HUVEC cells. (b) Phase contrast image showing cell morphology in each case along with stained nucleus. (c) Merged composition of panels a and b. (d) Quantitative estimation from different drug treatments using the mean fluorescence intensity variation of pixel data. (e) Typical z-stack image that is used for quantitative analysis. (f) Intracellular SWCNT concentrations from cell lysates obtained after various drug treatments. In agreement with fluorescence data, cytochalasin D induces the highest level of SWCNT uptake inhibition.

shown in Figure 2a–c, and also from the mean fluorescence intensity variation of pixel data, Figure 2d, we note that nocodazole and nystatin do not influence the DNA-SWCNT uptake significantly, whereas amiloride and chlorpromazine have a comparable effect (85 and 69% of the control, respectively). Moreover, cytochalasin D treatment significantly inhibits DNA-SWCNT cellular uptake (18% of the control, Figure 2d). In an independent experiment, intracellular SWCNT concentrations were monitored by UV/vis absorbance spectroscopy of cell lysate (Figure 2f). These confirm a distinct difference (albeit smaller in magnitude) between amiloride, cytochalasin D, and control samples (Figure 2f). There is some uncertainty about the relationship between fluorescence intensity and SWCNT concentration. The former depends on the extent to which 5'-FAM-DNA remains conjugated to SWCNT for separation of the fluorophore from the SWCNT vicinity will presumably increase its yield. However, if one assumes that DNA removal from SWCNT is about the same under all conditions (recall that the drugs are removed prior to exposure of cells to DNA-SWCNT) we expect relative fluorescence intensity to approximately represent relative amounts of SWCNT internalized. Furthermore, agreement of trends with the independent UV/vis absorbance measurements gives additional confidence that this relative comparison is valid. Interestingly, intracellular concentrations, measured by absorbance intensities, exceed that of the incubation media, demonstrating that an active process of SWCNT accumulation is operative.

To interrogate independently whether DNA-SWCNT internalization operates by an actin polymerization-mediated pathway, a gene-knockout technique was employed. Macropinocytosis is known to be associated with the activation of Rho GTPases, such as Rac1 and Cdc42, which are responsible for triggering membrane ruffles by actin polymerization.<sup>45</sup> Therefore we have tested the role of Rac1 by use of a dominant negative Rac1 (Rac1-T17DN)<sup>46</sup> retrovirus. Retrovirus preparation and HUVEC infection with retrovirus are carried out as described previously.<sup>47,48</sup> The fragments encoding the genes are subcloned to a retroviral vector pMMP.<sup>47</sup> Upon infection, it turns off the actin mediated endocytotic mechanism. Rac1-T17DN expression is confirmed with the uptake of FITC conjugated dextran, MW 4000 (Dex 4k), and dextran, MW 70 000 (Dex-70k), indicating that the expression of Rac1-T17DN inhibited macropinocytosis. In Figure 3, we show that this method inhibited the internalization of DNA-SWCNT into cells by 90% compared with that of pMMP control vector.

Hence, using well-controlled DNA-SWCNT hybrids and by studying the effect of a number of mechanism-specific inhibitors, we demonstrated clearly that internalization of these hybrids into HUVEC cells is by macropinocytosis-mediated endocytosis, more specifically by actin polymerization based endocytosis. This observation is confirmed by retrovirus infection that independently blocks the same mechanism. Understanding the mechanism of SWCNT uptake in this manner is of importance both for the development of SWCNT-based biomedical technologies such as imaging, sensors, and



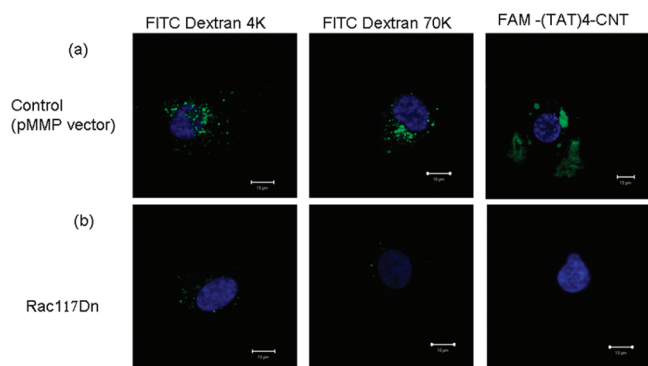


**Figure 3.** Rac1 controls the DNA-SWCNT uptake. (a) Fluorescence micrographs illustrating the uptake of dex 4k, dex 70k, and DNA-SWCNT (from left to right) in HUVEC cells that are treated with retrovirus containing pMMP control vector. (b) After treatment with Rac1-T17DN, uptake of the same respective molecules is inhibited.

drug delivery. Finally, this evidence serves to address fundamental issues related to their toxicity.

**Methods.** *SWCNT Preparation.* Raw (6,5)-rich (>80%) CoMoCAT carbon nanotubes, obtained from South West NanoTechnologies (SWeNT), and oligo-DNA sequence (TAT)<sub>4</sub> (selected for its ability to recognize the (6,5)-SWCNT),<sup>49</sup> obtained from Integrated DNA Technologies (IDT), were used throughout the study. They were sonicated in a 1 mg/1 mg weight ratio using a Branson probe ultrasonicator for 90 min at 8 W output power in 4 mL of 1xPBS buffer. For fluorescence studies, DNA was modified with a 5'-FAM fluorescent tag. All chemicals other than SWCNTs and DNA were purchased from Sigma-Aldrich. The resultant dispersion was centrifuged (Eppendorf microcentrifuge) for 90 min at 16000g to precipitate any undispersed CNTs and heavy-metal catalyst particles. Concentrations of (6,5) CNTs in solution were found by optical absorbance (Varian Cary 50 Spectrophotometer) at the E<sub>11</sub> transition, A<sub>990</sub> nm, using the ratio of 13 μg/mL CNT for 1.0 absorbance at 990 nm.<sup>50</sup> The resulting dispersion contained SWCNT with diameters in the range 0.7–0.9 nm and lengths in the range 100–500 nm.

*Cell Culture.* HUVECs were used throughout the study. HUVECs were cultured as described previously.<sup>47</sup> Briefly, HUVECs were grown on 30 μg/mL collagen-coated dishes in EGM-MV bullet kit (5% fetal bovine serum in EBM with 12 μg/mL bovine brain extract, 1 μg/mL hydrocortisone, and 1 μg/mL GA-1000) purchased from Cambrex Bio Science Walkersville, Inc., MD, U.S.A., in a humidified atmosphere with 5% CO<sub>2</sub> at 37 °C. HUVECs (passage 4) that were ~80% confluent were used for most experiments.

*Transmission Electron Microscopy Study.* TEM was used to examine CNTs inside the cell. On 60 mm collagen coated dishes,  $1.7 \times 10^5$  cells were plated and allowed to grow overnight in the incubator. Cells were then collected after treatment with 2 μg SWCNT/mL for 6 h and being resuspended in Trump's fixative solution, composed of 4 vol % formaldehyde and 1 vol % glutaraldehyde in 0.1 M phosphate buffer at pH 7.2. Then the cells were subjected to several washes with 0.1 M phosphate buffer, 1% osmium tetroxide in 0.1 M phosphate buffer, distilled water, 2 vol % uranyl acetate, distilled water, ethanol, and absolute acetone in sequence. Finally cells were put into resin and a resin block was prepared. The resin block was sliced to prepare the TEM grid, which was examined using a Philips Technai T12.

*Following Uptake by Confocal Fluorescence Microscopy and UV-vis Optical Spectroscopy.* Four common endocytotic pathways were investigated using pharmacological inhibitors. The associated mechanism and treatment conditions for these inhibitors are described in Supporting Information, Table S1. HUVEC cells were pretreated with these inhibitors for a specified duration. Then, the inhibitors were removed and the cells were exposed to DNA-SWCNT suspension. Cells were plated in a 60 mm collagen-coated dish for absorption measurement and were separately cultured under otherwise identical conditions on collagen coated cover glass slides for study by confocal microscopy. Uptake was quantified by UV/vis spectroscopy for which HUVEC cells were incubated with (TAT)<sub>4</sub>-conjugated SWCNT hybrids. Approximately  $1.7 \times 10^5$  cells were plated and allowed to grow overnight in the incubator. A concentration of 2 μg/mL of SWCNTs was used for various periods of time in the range, 0–6 h. After incubation, the cells were lysed with RIPA buffer mixed with PIC and HALT (Boston BioProducts). Cellular lysates from the longer incubation times appear to have pellets of aggregate CNTs. In order to redisperse the CNTs individually, 1 mL of a 0.2 wt % surfactant solution, sodium dodecylbenzene sulfonate (SDBS) was added to each sample, which was sonicated for 10 min using the same apparatus as before. The resultant lysates were again scanned using the spectrophotometer to measure absorbance at 990 nm, and accounting for dilutions, concentrations were obtained. For the confocal microscopy study, 5'-FAM was fused to (TAT)<sub>4</sub> to visualize its location inside the cells. After 6 h of exposure of 5'-FAM-(TAT)<sub>4</sub>-SWCNT, cells were processed for confocal study. Briefly, HUVEC cells were thoroughly washed with 1xPBS to exclude any presence of SWCNTs outside the cells as well as from the culture plates. They were then fixed with paraformaldehyde followed by three 1xPBS washes. The cells were then mounted with mounting medium containing DAPI (a blue dye used to stain the nuclei) on a glass slides and examined with a Zeiss LSM 780 microscope using 100× lens.

## ■ ASSOCIATED CONTENT

### § Supporting Information

Data from length-sorted DNA-SWCNT cellular toxicity studies as well as kinetics of cellular uptake. Further details on pharmacological inhibition parameters. Finally, interactions between DNA-SWCNT and cell media were examined. This material is available free of charge via the Internet at <http://pubs.acs.org>.

## ■ AUTHOR INFORMATION

### Corresponding Author

\*(A.J.) E-mail: [anj6@lehigh.edu](mailto:anj6@lehigh.edu). Phone: 610-758-4396. (D.M.) E-mail: [mukhopadhyay.debabrata@mayo.edu](mailto:mukhopadhyay.debabrata@mayo.edu). Phone: 507-538-3581.

### Notes

The authors declare no competing financial interest.

## ■ ACKNOWLEDGMENTS

This work was supported by National Institutes of Health (NIH) Grants HL70567 and CA150190, National Science Foundation (NSF) Grant CMMI-1014960, a Faculty Innovation Grant (FIG) to A.J. from Lehigh University, and a generous gift from Bruce and Martha Atwater to D.M. We also

acknowledge Jim Tarara, Mayo Clinic for helping us with confocal microscopy.

## REFERENCES

- (1) Prato, M.; Kostarelos, K.; Bianco, A. *Acc. Chem. Res.* **2008**, *41*, 60–68.
- (2) Liu, Z.; Tabakman, S. M.; Welscher, K.; Dai, H. *Nano Res.* **2009**, *2*, 85–120.
- (3) Chen, Z.; Tabakman, S. M.; Goodwin, A. P.; Kattah, M. G.; Daranciang, D.; Wang, X.; Zhang, G.; Li, G.; Liu, Z.; Utz, P. J.; Jiang, K.; Fan, S.; Dai, H. *Nat. Biotechnol.* **2008**, *26* (11), 1285–1292.
- (4) Liu, Z.; Chen, K.; Davis, C.; Sherlock, S.; Cao, Q.; Chen, X.; Dai, H. *Cancer Res.* **2008**, *68* (16), 6652–6660.
- (5) Zheng, M.; Jagota, A.; Semke, E. D.; Diner, B. A.; Mclean, S. R. L.; Richardson, R. E.; Tassi, N. G. *Nat. Mater.* **2003**, *2*, 338–343.
- (6) Liu, Z.; Winters, M.; Holodniy, M.; Dai, H. *Angew. Chem.* **2007**, *119*, 2069–2073.
- (7) Kam, N. W. S.; Liu, Z.; Dai, H. *J. Am. Chem. Soc.* **2005**, *127*, 12492–12493.
- (8) Kam, N. W. S.; Liu, Z.; Dai, H. *J. Am. Chem. Soc.* **2004**, *126*, 6850–6851.
- (9) Welscher, K.; Liu, Z.; Daranciang, D.; Dai, H. *Nano Lett.* **2008**, *8* (2), 586–590.
- (10) Heller, D. A.; Jin, H.; Martinez, B. M.; Patel, D.; Miller, B. M.; Yeung, T. K.; Jena, P. V.; Hobartner, C.; Ha, T.; Silverman, S. K.; Strano, M. S. *Nat. Nanotechnol.* **2008**, *4*, 114–120.
- (11) Strano, M. S.; Jin, H. *ACS Nano* **2008**, *2* (9), 1749–1752.
- (12) Liu, Z.; Li, X.; Tabakman, S. M.; Jiang, K.; Fan, S.; Dai, H. *J. Am. Chem. Soc.* **2008**, *130* (41), 13540–13541.
- (13) Zavaleta, C.; Zerda, A.; Keren, S.; Cheng, Z.; Schipper, M.; Chen, X.; Dai, H.; Gambhir, S. S. *Nano Lett.* **2008**, *8* (9), 2800–2805.
- (14) Zerda, A.; Zavaleta, C.; Keren, S.; Vaithilingam, S.; Bodapati, S.; Liu, Z.; Levi, J.; Smith, B. R.; Ma, T. J.; Oralkan, O.; Cheng, Z.; Chen, X.; Dai, H.; Khuri-Yakub, B. T.; Gambhir, S. S. *Nat. Nanotechnol.* **2008**, *3*, 557–562.
- (15) Liu, Z.; Davis, C.; Cai, W.; He, L.; Chen, X.; Dai, H. *Proc. Natl. Acad. Sci. U.S.A.* **2008**, *105* (5), 1410–1415.
- (16) Liu, Z.; Cai, W.; He, L.; Nakayama, N.; Chem, K.; Sun, X.; Chen, X.; Dai, H. *Nat. Nanotechnol.* **2007**, *2*, 47–52.
- (17) Poland, C. A.; Duffin, R.; Kinloch, I.; Maynard, A.; Wallace, W. A. H.; Seaton, A.; Stone, V.; Brown, S.; MacNee, W.; Donaldson, K. *Nat. Nanotechnol.* **2008**, *3*, 423–428.
- (18) Kostarelos, K. *Nat. Biotechnol.* **2008**, *26*, 774–776.
- (19) Warheit, D. B.; Laurence, B. R.; Reed, K. L.; Roach, D. H.; Reynolds, G. A. M.; Webb, T. R. *Toxicol. Sci.* **2003**, *77* (1), 117–125.
- (20) Stuart, L. M.; Ezekowitz, R. A. *Immunity* **2005**, *22* (5), 539–50.
- (21) Mellman, I. *Annu. Rev. Cell Dev. Biol.* **1996**, *12*, 575–625.
- (22) Conner, S. D.; Schmid, S. L. *Nature* **2003**, *422* (6927), 37–44.
- (23) Nichols, B. J. *Cell Sci.* **2003**, *116* (Pt 23), 4707–14.
- (24) Pelkmans, L.; Puntener, D.; Helenius, A. *Science* **2002**, *296* (5567), 535–9.
- (25) Ehrlich, M.; Boll, W.; Van Oijen, A.; Hariharan, R.; Chandran, K.; Nibert, M. L.; Kirchhausen, T. *Cell* **2004**, *118* (5), 591–605.
- (26) Swanson, J. A.; Watts, C. *Trends Cell Biol.* **1995**, *5* (11), 424–8.
- (27) Shi, X.; von dem Bussche, A.; Hurt, R. H.; Kane, A. B.; Gao, H. *Nature Nanotechnology* **2011**, *6*, 714–719.
- (28) Kam, N. W. S.; Liu, Z. A.; Dai, H. J. *Angew. Chem., Int. Ed.* **2006**, *45* (4), 577–581.
- (29) Jin, H.; Heller, D. A.; Strano, M. S. *Nano Lett.* **2008**, *8* (6), 1577–1585.
- (30) Jin, H.; Heller, D. A.; Sharma, R.; Strano, M. S. *ACS Nano* **2009**, *3* (1), 149–58.
- (31) Pantarotto, D.; Briand, J. P.; Prato, M.; Bianco, A. *Chem. Commun. (Cambridge, U.K.)* **2004**, *1*, 16–7.
- (32) Kostarelos, K.; Lacerda, L.; Pastorin, G.; Wu, W.; Wieckowski, S.; Luangsivilay, J.; Godefroy, S.; Pantarotto, D.; Briand, J. P.; Muller, S.; Prato, M.; Bianco, A. *Nat. Nanotechnol.* **2007**, *2* (2), 108–13.
- (33) Porter, A. E.; Gass, M.; Muller, K.; Skepper, J. N.; Midgley, P. A.; Welland, M. *Nat. Nanotechnol.* **2007**, *2* (11), 713–7.
- (34) Cherukuri, P.; Bachilo, S. M.; Litovsky, S. H.; Weisman, R. B. *J. Am. Chem. Soc.* **2004**, *126* (48), 15638–9.
- (35) Cai, D.; Mataraza, J. M.; Qin, Z. H.; Huang, Z.; Huang, J.; Chiles, T. C.; Carnahan, D.; Kempa, K.; Ren, Z. *Nat. Methods* **2005**, *2*, 449–454.
- (36) Heller, D. A.; Baik, S.; Eurell, T. E.; Strano, M. S. *Adv. Mater.* **2005**, *17* (23), 2793–2799.
- (37) Bahr, J. L.; Mikkelsen, E. T.; Bronikowski, M. J.; Smalley, R. E.; Tour, J. M. *Chem. Commun.* **2001**, 193–194.
- (38) Furtado, C. A.; Kim, U. J.; Gutierrez, H. R.; Pan, L.; Dickey, E. C.; Eklund, P. C. *J. Am. Chem. Soc.* **2004**, *126*, 6095–6105.
- (39) Boisvert, M.; Fernandes, S.; Tijssen, P. *J. Virol.* **2010**, *84* (15), 7782–92.
- (40) Hasebe, R.; Suzuki, T.; Makino, Y.; Igarashi, M.; Yamanouchi, S.; Maeda, A.; Horiuchi, M.; Sawa, H.; Kimura, T. *BMC Microbiol.* **2010**, *10*, 165.
- (41) Chen, Y.; Wang, S.; Lu, X.; Zhang, H.; Fu, Y.; Luo, Y. *Blood* **2011**, *117* (23), 6392–403.
- (42) West, M. A.; Bretscher, M. S.; Watts, C. *J. Cell Biol.* **1989**, *109* (6 Pt1), 2731–9.
- (43) Tremblay, P. L.; Auger, F. A.; Huot, J. *Oncogene* **2006**, *25* (50), 6563–73.
- (44) Sawyer, S. J.; Norvell, S. M.; Ponik, S. M.; Pavalko, F. M. *Am. J. Physiol. Cell Physiol.* **2001**, *281* (3), C1038–45.
- (45) Ridley, A. J.; Paterson, H. F.; Johnston, C. L.; Diekmann, D.; Hall, A. *Cell* **1992**, *70* (3), 401–10.
- (46) Zeng, H.; Zhao, D.; Mukhopadhyay, D. *J. Biol. Chem.* **2002**, *277* (48), 46791–8.
- (47) Zeng, H.; Dvorak, H. F.; Mukhopadhyay, D. *J. Biol. Chem.* **2001**, *276* (29), 26969–79.
- (48) Zeng, H.; Sanyal, S.; Mukhopadhyay, D. *J. Biol. Chem.* **2001**, *276* (35), 32714–9.
- (49) Tu, X. M.; Manohar, S.; Jagota, A.; Zheng, M. *Nature* **2009**, *460* (7252), 250–253.
- (50) Zheng, M.; Diner, B. A. *J. Am. Chem. Soc.* **2004**, *126*, 15490–15494.